

## Plasma damage effects on low-*k* porous organosilicate glass

H. Ren,<sup>1</sup> G. A. Antonelli,<sup>2</sup> Y. Nishi,<sup>3</sup> and J. L. Shohet<sup>1,a)</sup>

<sup>1</sup>Department of Electrical and Computer Engineering, Plasma Processing and Technology Laboratory, University of Wisconsin–Madison, Madison, Wisconsin 53706, USA

<sup>2</sup>Novellus Systems, Tualatin, Oregon 97062, USA

<sup>3</sup>Stanford University, Stanford, California 94305, USA

(Received 30 July 2010; accepted 27 September 2010; published online 9 November 2010)

Damage induced in low-*k* porous organosilicate glass (SiCOH) dielectric films by exposure to an electron cyclotron resonance (ECR) plasma was investigated. The effects of charged-particle bombardment and vacuum ultraviolet radiation were separated. Flux measurements showed that the ECR plasma has a greater photon flux in the vacuum ultraviolet (VUV) range than in the UV range. Damage was measured by examining the surface potential and capacitance-voltage characteristics after exposure. It was found that during argon ECR plasma processing, 75% of the charge accumulation comes from ions at the surface, while 25% of the charge accumulation occurs from charge trapped within the bulk of the dielectric film. The charge accumulation can be modified by changing the bias voltage of the wafer chuck. UV exposure was shown to repair both sources of damage. Fourier transform infrared (FTIR) spectroscopy results showed no significant change except for Si-(CH<sub>3</sub>)<sub>x</sub> bonds. It was found that both charged-particle bombardment and radiation from the ECR plasma damage these bonds. Ellipsometric measurements showed that both the dielectric thickness and the dielectric constant changed during plasma exposure. In addition, both plasma-induced swelling and UV-exposure shrinking effects were observed. The plasma-induced swelling occurs at the surface of the dielectric without changing the porosity of the dielectric, while UV-induced shrinking changes the porosity significantly. © 2010 American Institute of Physics. [doi:10.1063/1.3506523]

### I. INTRODUCTION

During the plasma processing of microelectronic devices, dielectric materials are often damaged.<sup>1,2</sup> The damage results in the accumulation of trapped charges and an increase in defect-state concentrations. This leads to large leakage currents and jeopardizes the electrical reliability of devices.<sup>3</sup> Also, mechanical/chemical damages take place that result in undesirable deviations from the expected physical properties of the dielectric film.<sup>4</sup>

Low-*k* porous dielectrics, as alternatives for traditional SiO<sub>2</sub> films, have been investigated extensively.<sup>5,6</sup> For example, organosilicate glass (SiCOH) is recognized as a promising low-*k* porous dielectric.<sup>7</sup> However, during plasma processing of SiCOH dielectrics, damage has been observed.<sup>8,9</sup> The damage primarily comes from charged-particle bombardment and plasma radiation.<sup>10</sup> Hence, an investigation of the mechanisms of these two effects is important in order to determine the damage levels and the potential for curing the damage.

In this work, we investigate the damage effects of electron cyclotron resonance (ECR) argon plasma exposure to SiCOH dielectric films. ECR systems can be used for deposition,<sup>11</sup> etching,<sup>12</sup> sputtering,<sup>13</sup> and ashing.<sup>11</sup> A capillary-array window was used to separate the plasma radiation from charged-particle bombardment. The capillary array window is able to shield out most of the particles while

letting the plasma radiation through.<sup>14</sup> Examination of the electrical, chemical, and mechanical properties can then be made while separating the two processes.

### II. EXPERIMENT

#### A. ECR plasma system

Figure 1 shows the schematic diagram of the ECR plasma system. The wafer chuck is 20 cm in diameter and is covered with Kapton tape except for the area that makes contact with the dielectric sample. The dielectric sample is attached to the wafer chuck with double-sided conductive tape. The substrate can be biased negatively while measuring the current during plasma exposure with a picoammeter. Ar-

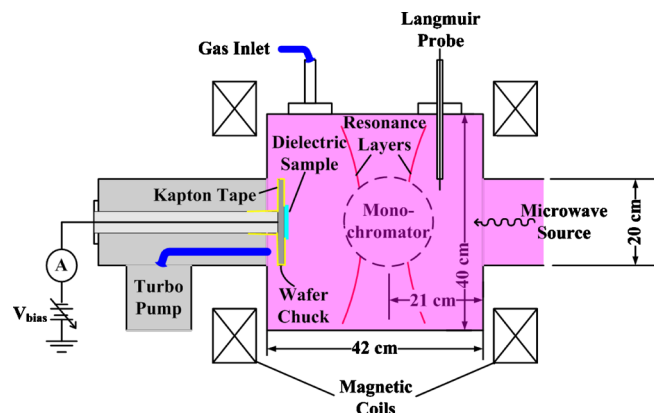


FIG. 1. (Color online) Schematic diagram of ECR plasma system.

<sup>a)</sup>Electronic mail: shohet@engr.wisc.edu.

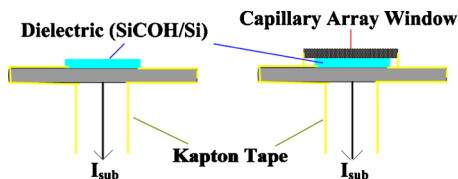


FIG. 2. (Color online) Arrangement of the SiCOH dielectric samples and the capillary array window.

gon gas is fed in at the top of the  $42 \times 40$  cm<sup>2</sup> vacuum chamber. ECR plasma forms with the synergism of the static magnetic field and a 2.45 GHz microwave source. A monochromator is connected to the chamber and is able to measure the vacuum ultraviolet (VUV) spectrum with a wavelength range from 50 to 300 nm. A Langmuir probe is used to measure the electron density and electron temperature. These quantities are used as input to a code that calculates the photon spectrum emitted from the plasma.<sup>15</sup>

### B. Plasma exposure of the SiCOH dielectric samples

ECR plasma exposure was made on two SiCOH dielectric samples. The SiCOH dielectric films were plasma-enhanced-chemical-vapor-deposited on a silicon substrate with a thickness of 200 nm and dielectric constant  $k=2.65$ . Figure 2 shows the arrangement of the SiCOH dielectric samples on the wafer chuck. Each sample was attached to the wafer chuck with conductive tape. One of the samples was covered with the capillary-array window to keep particles from traveling to the sample while allowing VUV photons to pass through.<sup>14</sup> The uncovered area of the wafer chuck was covered with Kapton tape such that no plasma-wafer-chuck contact took place during exposure. Thus, any measured substrate currents are totally due to the plasma effects on dielectric samples. In order to maintain the same processing condition, both samples were exposed simultaneously. However, separate exposures for the covered and uncovered samples were also made to verify the results.

The samples were exposed to an ECR plasma under the same conditions: 400 W 2.45 GHz microwave power, 5 mTorr argon neutral pressure,  $-20$  V bias on the wafer chuck, and 12 min of exposure time. Some of the samples were also exposed to UV with a 4.9 eV HgAr lamp in air after plasma exposure to investigate the possibility of damage repair.

As mentioned above, the capillary-array window can shield out charged-particle bombardments and let the plasma radiation through. This allows for a separation of the particle and photon bombardment effects. That is, the sample covered with the capillary array window only receives plasma radiation while the sample without the capillary array window is subject to the both particle bombardment and plasma radiation. The capillary array window is approximately 90% transparent to the plasma radiation<sup>14</sup> and this factor was taken into account.

### C. Characterization of dielectric properties

Three dielectric properties are considered: (1) electrical properties (i.e., charge accumulation within the dielectric and

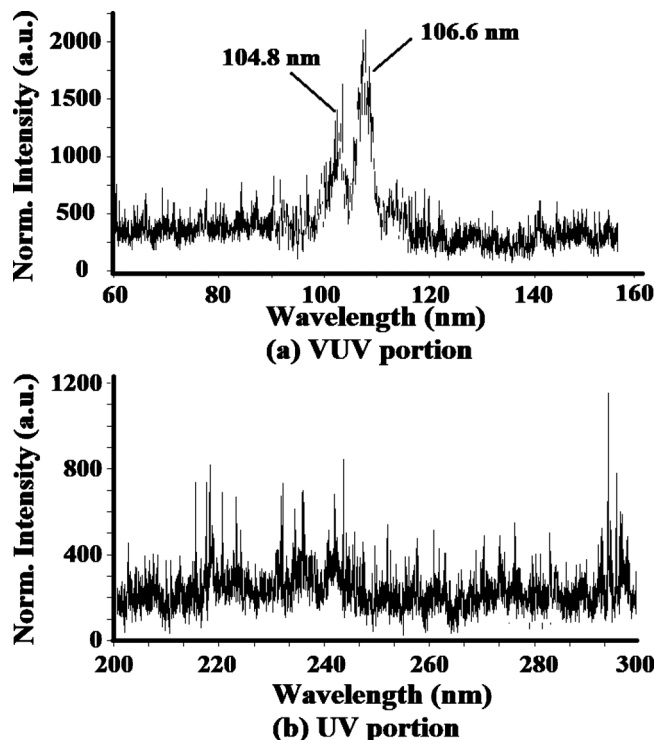


FIG. 3. VUV and UV portions of the ECR argon plasma spectrum.

leakage current), (2) chemical properties, and (3) physical properties including modifications of thickness and porosity of the dielectrics.

To investigate the electrical properties, the surface potential of the dielectric was measured with a Kelvin probe and the capacitance-voltage (C-V) characteristics were measured with a mercury probe. The surface potential is a function of the total amount of charge accumulation in the dielectric.<sup>16</sup> The flat-band voltage shift in the C-V characteristics shows the change in the amount of trapped charges within the dielectric.<sup>17</sup> In addition, the surface potential decay after the plasma exposure can be measured to determine the magnitude of the leakage current.

For chemical property measurements, Fourier transform infrared spectroscopy (FTIR) was used. Multiple chemical bonds were identified: Si-(CH<sub>3</sub>)<sub>x=1,2, or 3</sub> at 700–900 cm<sup>-1</sup>, Si-O stretch band at 970–1250 cm<sup>-1</sup>, Si-CH<sub>3</sub> at 1274 cm<sup>-1</sup>, C=O at 1710 cm<sup>-1</sup>, Si-H at 2220 cm<sup>-1</sup>, and CH<sub>x</sub> at 2970 cm<sup>-1</sup>.<sup>7,18</sup>

For thickness and porosity measurements of the dielectrics, a three-color ellipsometer (blue at 405.0 nm, green at 546.1 nm, and red at 632.8 nm) was used. The change in thickness of the dielectrics for various exposure conditions was measured. In addition, changes in the porosities can be determined using the same ellipsometer.<sup>19</sup>

## III. RESULTS AND DISCUSSION

### A. Plasma radiation spectrum

Figure 3 shows the spectrum of the ECR argon plasma measured with a calibrated monochromator. Strong VUV argon lines at 104.8 and 106.6 nm were observed. Also, it is seen from the normalized intensities of the spectrum that the

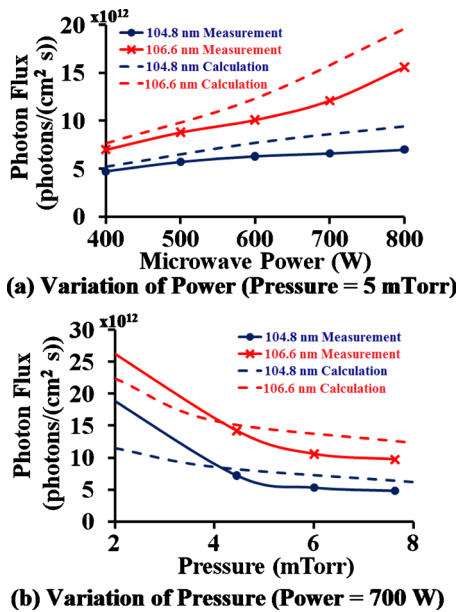


FIG. 4. (Color online) Comparison of measured and calculated VUV photon fluxes as functions of microwave power and neutral pressure.

VUV lines have much higher intensities than the UV lines. Figure 4 shows estimated results of the photon flux densities as functions of plasma conditions. From Fig. 4, it is seen that the measurements and code calculations results match well and the VUV photon flux rates from the plasma are on the order of  $10^{13}$  photons/( $\text{cm}^2$  s).

## B. Processing-induced charge accumulation

In order to investigate the charge accumulation mechanisms in detail, surface potentials were measured before and after processing for the samples with and without the capillary array window. Figure 5 shows the surface potential results. It is shown that before the processing, the two samples have the same surface potential level ( $\sim 0$  V). After 12 min of processing, the samples with and without the capillary window charge up to different surface potentials. (8.5 V and 7.2 V, respectively) In addition, the surface-potential decay rates of the samples after exposure are different. The surface potential of the sample that is not covered by the window shows a faster decay and reaches a steady value of 1.1 V three hours after plasma exposure. The surface potential of the sample with the window decays slowly down to 2.3 V after 12 h after processing. This interesting phenomenon leads to

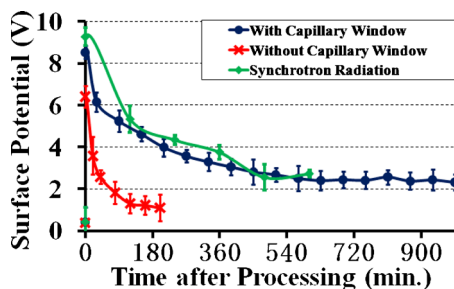


FIG. 5. (Color online) Surface potential decay after plasma exposure for dielectrics with/without the capillary array window compared with synchrotron radiation exposure at 10 eV.

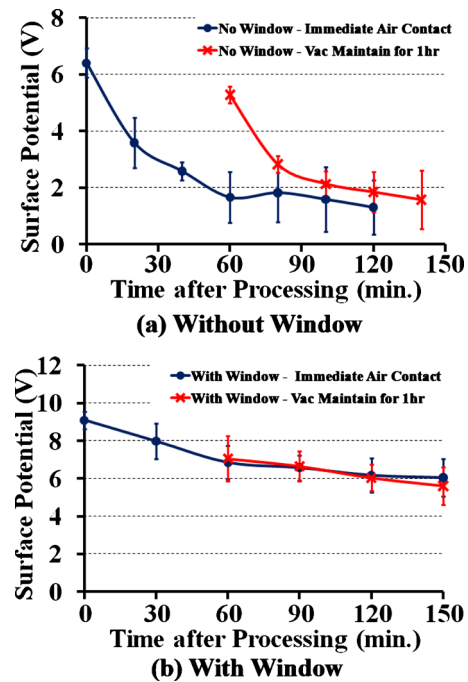


FIG. 6. (Color online) Comparison of the surface potential decay with and without a 1 h vacuum hold after plasma exposure for dielectrics with and without the capillary-array window.

the likelihood of there being different mechanisms of charge accumulation from particle bombardment and from radiation bombardment. From previous work, we showed that VUV exposure accumulates trapped charges within the dielectric layers by various photon processes.<sup>20</sup> This charge accumulation happens deep within the dielectric and is neutralized over time by the leakage current through the dielectric layer. To confirm this, a separate 10 eV VUV exposure was made at the University of Wisconsin Synchrotron Center. The photon flux of the VUV exposure was set to be at the same level as the plasma radiation. From Fig. 5, we show that the decay rates after synchrotron radiation and plasma radiation (the case with the window) are roughly the same. Hence, the charge accumulation mechanism of the window-covered sample due to photon bombardment and not from particles that might have been able to pass through the capillary-array window.

For the sample that is not covered by the window, we hypothesize that the rapid decay of the surface potential is due to contact with the air of the ions implanted on the surface. In order to verify this, vacuum environment was maintained for one hour after the processing was made. The surface potential decays were measured for plasma exposure with and without the capillary-array window. The results are shown in Fig. 6. It is seen in Fig. 6(a) that with the vacuum maintained, the surface potential of the uncovered sample does not decay as rapidly during the same time period. This indicates that the vacuum helps prevent the surface potential from decaying for the sample that was directly exposed to the plasma. Thus we conclude that one mechanism of charge accumulation for plasma-exposed sample (without the capillary-array window) is surface ion sticking. In contrast Fig. 6(b) shows the same decay rate for the sample covered

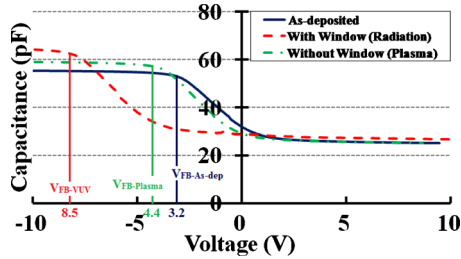


FIG. 7. (Color online) C-V characteristics of the dielectric samples. (The surface potential increases for the samples with and without the capillary-array window are 6.3 V and 4.6 V, respectively.)

with the capillary-array window no matter whether or not the sample is kept under vacuum. This indicates the leakage-current-induced charge decay happens within the dielectric and does not depend on the vacuum/air environment.

In order to quantitatively separate the two mechanisms of charge accumulations, C-V measurements were made on the samples as shown in Fig. 7. The surface sticking ions will instantaneously disappear when they make contact with the mercury drop of the probe, leaving only the trapped charges within the dielectric that are generated by photon bombardment. The C-V characteristics were measured for the as-is sample (a pristine sample with no treatment) and the samples with/without the capillary-array window after plasma exposure. Thus, both charge accumulation processes change the surface potential. However, charge trapped within the dielectric produces a flat-band voltage shift as well as a change in surface potential, while charge that is accumulated on the dielectric vacuum surface while also resulting in a change in surface potential does not produce a flat-band voltage shift. This is because the mercury probe drains the surface charges when it is in contact with the surface. Hence, to ensure that all charge was considered, the surface potential was measured before and after the C-V characteristics were taken.

For the window-covered sample, a surface-potential increase of 6.3 V was obtained before the C-V characteristics were taken while the flatband voltage shift was 5.5 V. The surface potential after the C-V characteristics were taken was about 5.6 V, thus showing that the flatband voltage shift is roughly equivalent to the surface potential. For this sample, this result indicates that most (>85%) of the plasma radiation produces trapped charge accumulation within the dielectric layer and is detectable from the C-V characteristics. For the uncovered sample, the surface potential increase was 4.6 V while the flatband voltage shift was 1.2 V with a corresponding decrease in surface potential after the C-V characteristics were measured. This indicates that less than 30% of the plasma-induced charge accumulation is due to trapped charges within the dielectric. Thus, we conclude that the remaining 70% of the charge accumulation is due to ion sticking at the dielectric surface. Based on this, we believe that all trapped-charge accumulation during plasma exposure is due to photon bombardment as long as the wafer bias is relatively low in order to eliminate ion implantation well below the surface. For low bias of  $-20$  V, the ratio of the ion-bombardment to photon bombardment on charge accumulation is around 3:1.

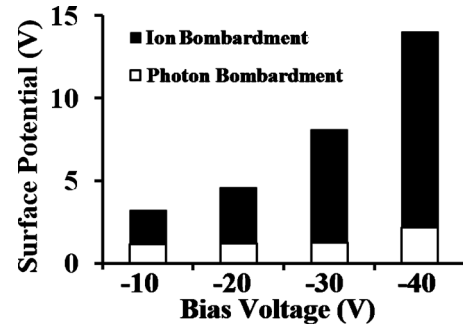


FIG. 8. Contributions to the plasma-induced charge accumulation for different substrate bias voltages.

The above results were obtained for a substrate bias voltage of  $-20$  V. To verify our assumption, different bias voltages were used to measure the particle and photon bombardment effects on charge accumulation. Figure 8 shows the contributions of the ion and photon bombardment to the surface potential for different substrate bias voltages. It is seen that as the amplitude of the negative bias voltage increases, ion bombardment results in more charge accumulation while the charge accumulation from photon bombardment remains about the same.

To repair the charging damage, a 4.9 eV HgAr UV lamp exposure on the sample was able to repair the charge accumulation due to VUV radiation by electron repopulation.<sup>20</sup> The HgAr lamp curing effects on the plasma exposure-induced charge accumulation were also examined. After exposure, the UV lamp irradiated the samples for 1 min (a fluence of  $6 \times 10^{13}$  photons/cm<sup>2</sup>). Figure 9 shows that, with UV exposure, the surface potentials decrease back to zero. Thus UV exposure heals both particle and photon bombardment charge accumulation.

### C. Chemical bond concentrations

Figure 10 shows the FTIR results on as-deposited sample and processed samples with and without the capillary array window. It is seen that unlike plasma with reactive gases,<sup>10</sup> no significant changes in the chemical bonds take place except for the Si-(CH<sub>3</sub>)<sub>x</sub> bonds. From Fig. 10, FTIR shows that the Si-(CH<sub>3</sub>)<sub>x</sub> bond concentrations increase due to plasma photon bombardment. The concentration is higher for the uncovered sample showing that plasma exposure also increases the Si-(CH<sub>3</sub>)<sub>x</sub> concentration by ion bombardment. It is important to note that the increase in the Si-(CH<sub>3</sub>)<sub>x</sub> wagging bond concentration does not indicate any chemical reaction taking place. It only indicates that during the pro-

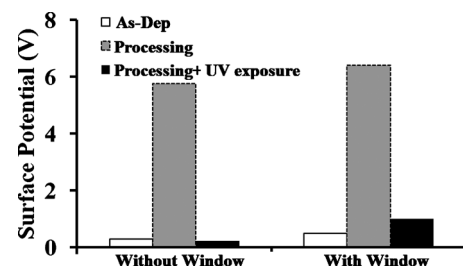


FIG. 9. UV-lamp curing for plasma-induced charge accumulation.

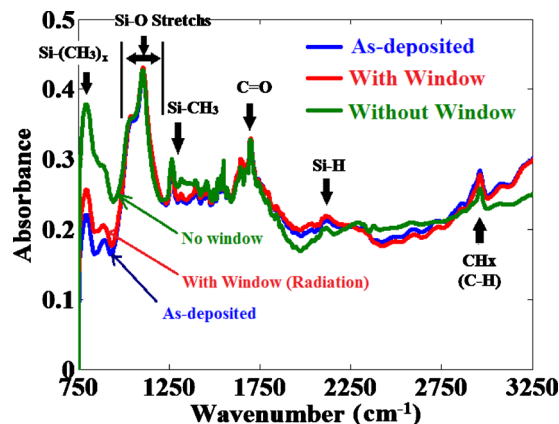


FIG. 10. (Color online) Fourier transform infrared measurements of as-is and with and without capillary-array window after plasma exposure.

cessing, the dielectric film was subject to physical change so that a more twisted bonding structure was seen.

#### D. Dielectric thickness and porosity

Dielectric thicknesses and dielectric constants were measured with a three-color ellipsometer. Figure 11 shows that plasma processing has a small swelling effect (2.4 nm increase) on the dielectric thickness while UV exposure has a significant shrinking effect (30 nm). The dielectric constant is unchanged due to plasma exposure but does increase after UV.

The swelling effect from plasma exposure is likely due to the collection of a large number of ions on the surface because of the substrate bias. The 2.4 nm of thickness increase is equivalent to approximately ten argon-ion monolayers on the dielectric surface. In addition, according to the relationship between the surface potential and charge accumulation,<sup>21</sup> the amount of sticking argon ions per unit area is calculated as  $1.8 \times 10^{12}$  ions/cm<sup>2</sup> which is approxi-

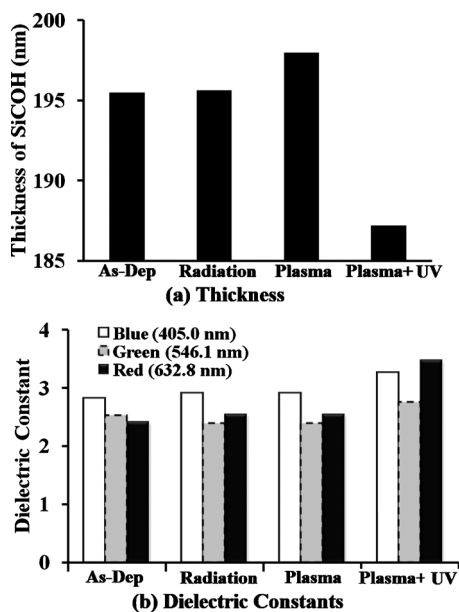


FIG. 11. Modification of dielectric thickness and dielectric constant due to photon bombardment, plasma exposure, and UV-lamp curing.

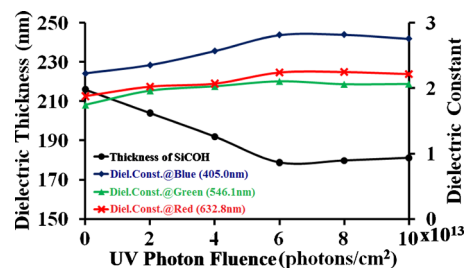


FIG. 12. (Color online) UV shrinking effect of SiCOH dielectric as a function of UV photon fluence.

mately six monolayers if the ions are closely packed. In addition, ellipsometry measurements made after the mercury drop was in contact with the dielectric during the C-V characteristic measurements, showed that the thickness decreased back to the level it was before plasma exposure. Hence, the swelling effect is likely due to ion sticking at the surface and does not influence the dielectric constant.

The UV shrinking effect has been proposed to be mainly due to chemical condensation.<sup>22</sup> Here it is investigated as a function of UV photon density. It is seen in Fig. 12 that as the UV photon density increases, the thickness of the SiCOH dielectric layer decreases until it reaches a steady value. Meanwhile, the dielectric constants measured at the three colors used in the ellipsometer increase. This indicates that after UV exposure, the dielectric sample becomes less porous. Although UV curing can cure the charge accumulation of the dielectric, because of the change in thickness and dielectric constants, it can cause physical damage to the dielectric and make the dielectric less porous.

#### IV. CONCLUSION

Using a capillary-array window, it is now possible to separate particle-bombardment and plasma-radiation effects during ECR plasma exposure on SiCOH. It was found that plasma-induced charge accumulation has two parts: surface ion sticking due to ion bombardment and trapped-charge accumulation within the dielectric due to photon bombardment. Both charge accumulations can be cured by a 4.9 eV UV lamp. For ECR argon plasma exposure, the Si-(CH<sub>3</sub>)<sub>x</sub> bond concentrations are modified. In addition, plasma exposure results in a small swelling effect that is caused by ion sticking to the surface. UV lamp exposure has a significant shrinking effect and makes the dielectric less porous and thus should be carefully used.

#### ACKNOWLEDGMENTS

This work is supported by the Semiconductor Research Corporation under Contract No. 2008-KJ-1781. The UW Synchrotron is supported by NSF Grant No. DMR-0084402.

<sup>1</sup>J. Bao, H. Shi, J. Liu, H. Huang, P. S. Ho, M. D. Goodner, M. Moinpour, and G. M. Klooster, *J. Vac. Sci. Technol. B* **26**, 219 (2008).

<sup>2</sup>J. Kim, S. Kim, H. Jeon, M. H. Cho, K. B. Chung, and C. Bae, *Appl. Phys. Lett.* **87**, 053108 (2005).

<sup>3</sup>K. P. Cheung, *Plasma Charging Damage* (Springer-Verlag, Berlin, Germany, 2000).

<sup>4</sup>D. Rats, V. Hajek, and L. Martinu, *Thin Solid Films* **340**, 33 (1999).

<sup>5</sup>B. P. Gorman, R. A. Orzco-Teran, J. A. Roepsch, H. Dong, and D. W.

- Mueller, *Appl. Phys. Lett.* **79**, 4010 (2001).
- <sup>6</sup>Y. H. Kim, S. K. Lee, and H. J. Kim, *J. Vac. Sci. Technol. A* **18**, 1216 (2000).
- <sup>7</sup>A. Grill, *J. Appl. Phys.* **93**, 1785 (2003).
- <sup>8</sup>H. Cui, R. J. Carter, D. L. Moore, H.-G. Peng, D. W. Gidley, and P. A. Burke, *J. Appl. Phys.* **97**, 113302 (2005).
- <sup>9</sup>A. Grill and V. Patel, *J. Electrochem. Soc.* **153**, F169 (2006).
- <sup>10</sup>S. Uchida, S. Takashima, M. Hori, M. Fukasawa, K. Ohshima, K. Nagahata, and T. Tatsumi, *J. Appl. Phys.* **103**, 073303 (2008).
- <sup>11</sup>Y. H. Shing, *Sol. Cells* **27**, 331 (1989).
- <sup>12</sup>K. Xie, J. R. Flemish, J. H. Zhao, W. R. Buchwald, and L. Casas, *Appl. Phys. Lett.* **67**, 368 (1995).
- <sup>13</sup>S. Hirono, H. Torii, T. Tajima, T. Amazawa, S. Umemura, T. Kamata, and Y. Hirabayashi, *Mater. Sci. Forum* **645–648**, 725 (2010).
- <sup>14</sup>J. D. Chatterton, G. S. Upadhyaya, J. L. Shohet, J. L. Lauer, R. D. Bathke, and K. Kukkady, *J. Appl. Phys.* **100**, 043306 (2006).
- <sup>15</sup>C. Cismaru and J. L. Shohet, *Appl. Phys. Lett.* **74**, 2599 (1999).
- <sup>16</sup>J. L. Lauer and J. L. Shohet, *IEEE Trans. Plasma Sci.* **33**, 248 (2005).
- <sup>17</sup>H. Sinha, J. L. Lauer, M. T. Nichols, G. A. Antonelli, Y. Nishi, and J. L. Shohet, *Appl. Phys. Lett.* **96**, 052901 (2010).
- <sup>18</sup>M. Darnon, T. Chevolleau, T. David, N. Posseme, J. Ducote, C. Licitra, L. Vallier, O. Joubert, and J. Torres, *J. Vac. Sci. Technol. B* **26**, 1964 (2008).
- <sup>19</sup>M. R. Baklanov, K. P. Mogilnikov, V. G. Polovinkin, and F. N. Dultsev, *J. Vac. Sci. Technol. B* **18**, 1385 (2000).
- <sup>20</sup>J. L. Lauer, H. Sinha, M. T. Nichols, G. A. Antonelli, Y. Nishi, and J. L. Shohet, *J. Electrochem. Soc.* **157**, G177 (2010).
- <sup>21</sup>H. Ren, H. Sinha, A. Sehgal, M. T. Nichols, G. A. Antonelli, Y. Nishi, and J. L. Shohet, *Appl. Phys. Lett.* **97**, 072901 (2010).
- <sup>22</sup>J. Y. Zhang and I. W. Boyd, *Mater. Sci. Semicond. Process.* **3**, 345 (2000).